

# Synthesis of Phase-Pure Zeolite Sodalite from Clear Solution Extracted from Coal Fly Ash

Hums E\*

Consulting Environmental Catalysis, PO Box 1848, 91008 Erlangen, Germany

## Abstract

The formation of zeolite sodalite (SOD) as a by-product in the synthesis of zeolite X from clear solution extracted from fused South African coal fly ash has recently been studied. However, the present study shows that zeolite X as well as zeolite A should be seen as intermediate structures and that phase-pure sodalite can be obtained by increasing crystallization time and temperature. To investigate the transition from zeolites A and X into SOD, the crystallization was conducted at 70, 80, and 90°C for different times. In addition to structural and chemical analyses by XRD and ICP, respectively, a detailed morphological characterization of the synthesis products by scanning electron microscopy (SEM) was undertaken in order to investigate the effect of the crystallization conditions on different crystal morphologies of zeolite SOD.

**Keywords:** Coal fly ash; Sodalite; Zeolite; Phase transformation

## Introduction

Coal-fired power plants accounted for 41% of the global electricity production in 2006 and are expected to reach 44% in 2030. Apart from activities to replace conventional energy from fossil fuel, coal consumption increased globally for the decade of 2002–2012. A total of 750 million tonnes of fly ash were produced globally in 2012. Around 31 million tonnes of fly ash are produced just in South Africa per year but only about 6% is recycled. With a focus on sustainable resource management, because of the high content of silica and alumina coal fly ash, it is of interest as suitable feedstock in the synthesis of high-value zeolitic material and therefore competing with zeolites made from pure industrial chemicals [1]. Hydroxysodalite  $\text{Na}_6[\text{AlSi}_4\text{O}_{16}(\text{OH})_2] \cdot 2\text{H}_2\text{O}$  (SOD) as well as zeolites X, Y (FAU) and zeolite A (LTA) belong to the class of zeolites which have the common characteristic of  $\beta$ -cages (sodalite units) as common building unit. Although it is well-known that sodalite can be ideally formed by direct attachment of sodalite units, there is still a constant interest to study the process of SOD synthesis. Sodalite can be successfully synthesized starting the crystallization either from gels [2], applying hydrothermal reaction conditions to mullite and quartz [3], or transformation of zeolite A [4]. Al-Azmi [5] found that the synthesis temperature and the amount of sodium hydroxide are the most important variables affecting the sodalite formation and the morphology when starting from gels. Furthermore, Huang et al. [6] mentioned that in zeolite A synthesis gel, which was free of structure-directing agents, nanocrystalline sodalite could be obtained when large amounts of ethanol were added. From this point of view, they systematically studied the crystallization of sodalite in the  $\text{NaOH}-\text{Al}_2\text{O}_3-\text{SiO}_2-\text{H}_2\text{O}$  system in the presence of ethanol. Structures with different morphologies were found. In particular, clusters of sodalite discs, spherical aggregates of sodalite nanoplates (e.g., thread-ball-like particles), and core-shell/hollow sodalite structures were synthesized by varying the ethanol content and hydrothermal synthesis time. In this context they reported, that zeolite A is more stable in a water solvent system, whereas the presence of ethanol accelerated phase transformation to sodalite. Early works published by Borchert and Keidel [7] and Barrer and White [8] opened the sodalite synthesis via hydrothermal conversion of kaolinite in the presence of sodium hydroxide at low temperatures, whereas Novembre et al. [9] investigated the solid state transformation of metakaolinite to basic sodalite in the presence of NaCl in a so-called high temperature

dry process synthesis route at 850°C and ambient pressure. Silica, alumina, and oxides of iron and calcium are the main constituent parts of coal fly ash. Therefore coal fly ash, which is a by-product of coal fired power plants, is an upcoming alternative to other industrial resources used for the synthesis of zeolites [10]. The fly ash which was used in the present study contained more than 70 wt.%  $\text{SiO}_2+\text{Al}_2\text{O}_3$  (defined as class F coal fly ash corresponding with ASTM C618) and predominantly contaminated with  $\text{Fe}_2\text{O}_3$  and low in lime. Although several methods are available to convert fly ash into zeolites, there are still technical and economical obstacles of products and processing at semi-industrial scale to be solved before successful commercialization. Besides the processing costs and low yields, the mobility of heavy and toxic elements in fly ashes in contrast to the synthesis from industrial pure chemicals are of particular relevance [11]. A simple way to obtain zeolites from fly ash is the conventional hydrothermal conversion of a mixture of fly ash and alkaline solution. In this way, fly ash conversion of about 50% into zeolite, especially P and/or hydroxysodalite, was reached as shown by Singer and Berkgaut [12] and Izidoro et al. [13]. But it seems hard from our point of view to remove the insoluble fly ash impurities from the produced zeolitic material. As an alternative to this procedure a mixture of fly ash and sodium hydroxide can be fused at 550°C in order to convert insoluble  $\text{SiO}_2$  and  $\text{Al}_2\text{O}_3$  in the fly ash into soluble sodium silicate and sodium aluminate. Before reacted under hydrothermal conditions the soluble sodium silicate and sodium aluminate can be separated from the insoluble fly ash constituents. The zeolites can subsequently be crystallized from this clear solution extract, which has to be additionally doped with an external solution of aluminate to adjust the Si/Al ratio for the synthesis of selected zeolite types [14]. Crystallization from clear solution yields much lower amounts of zeolite, but the zeolite product exhibits significantly higher purity compared to the conventional hydrothermal fly ash

\*Corresponding author: Hums E, Consulting Environmental Catalysis, PO Box 1848, 91008 Erlangen, Germany, Tel: +499131858; E-mail: [humseric@t-online.de](mailto:humseric@t-online.de)

Received June 15, 2017; Accepted June 20, 2017; Published June 26, 2017

Citation: Hums E (2017) Synthesis of Phase-Pure Zeolite Sodalite from Clear Solution Extracted from Coal Fly Ash. J Thermodyn Catal 8: 187. doi: [10.4172/2157-7544.1000187](https://doi.org/10.4172/2157-7544.1000187)

Copyright: © 2017 Hums E. This is an open-access article distributed under the terms of the Creative Commons Attribution License, which permits unrestricted use, distribution, and reproduction in any medium, provided the original author and source are credited.

treatment. The high temperature fusion step makes it very energy intensive, therefore the optional use of microwave-assisted heating for the conversion of fly ash should not remain unmentioned to produce zeolites [15,16], although homogenous heating of the reaction mixture is then difficult. More than 60 wt.% of sodalite were formed from coal fly ash in a 3 M NaOH medium in less than 1 hour heating time via microwave-assisted heating [16]. It was stated that synthesis conditions and yield of zeolites obtained are comparable to conventional hydrothermal treatment, but activation time can be drastically reduced using microwave technology. The phase fraction of sodalite containing impurities of zeolite A was determined by XRD measurements and increased with increasing the reaction time from 30 to 45 minutes, suggesting that sodalite is the more stable zeolite phase compared to zeolite A, which is also in agreement with the findings of Maldonado et al. [17]. In most fly ash based zeolite synthesis processes, pure water as solvent for NaOH is used [18-26]. When Musyoka et al. [27] used waste industrial brine solutions instead of pure water, hydroxy sodalite was formed in significant quantity contaminated with the remaining amount of unconverted mullite and hematite from the fly ash feedstock. This is not surprising because both cancrinite and sodalite can be formed in alkaline solution from zeolite A depending on the types of anions [27,28]. The mineral phases observed in a study suggested that  $\text{Cl}^-$  and  $\text{NO}_2^-$  direct the nucleation of sodalite, whereas  $\text{SO}_4^{2-}$  direct the nucleation of cancrinite. It was also mentioned that some anions, such as  $\text{NO}_3^-$  and  $\text{NO}_2^-$  can act as templates for both cancrinite and sodalite as discussed by Deng et al. [29]. Subotic et al. [30] worked out details of mechanistic aspects to synthesize hydroxy sodalite by transformation of zeolite A in the presence of concentrated solution of sodium hydroxide. From this point of view our interest was focused on sodalite which we recognized as contaminant when studying the kinetics of zeolite X formation based on in situ ultrasonic data starting from clear solution extracted from alkali fused coal fly ash [31]. The progress of attenuation of ultrasound during synthesis of zeolite X at different temperatures is shown in Figure 1. There, the crystallisation of zeolite X was already finished within 17 h in a temperature range between 80 and 94°C. It was the purpose of the present study to investigate further time- and temperature-dependent effects on zeolite X and SOD formation based on the former synthesis route published in [31] with the aim to examine formation and morphology of phase-pure SOD.

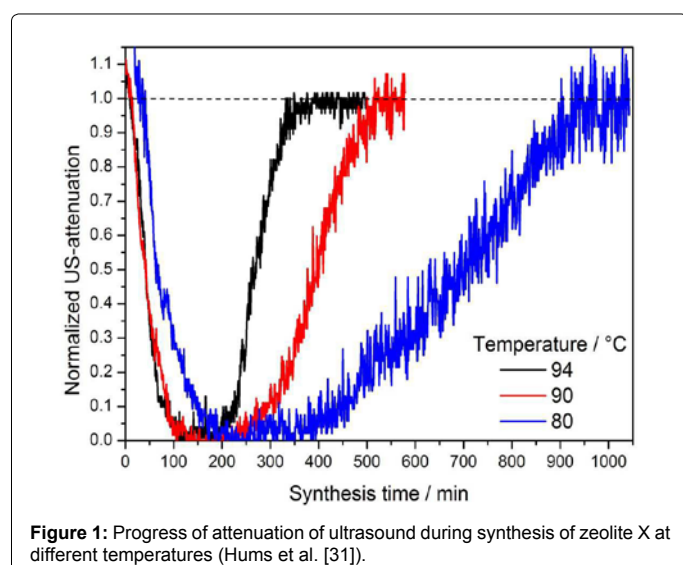


Figure 1: Progress of attenuation of ultrasound during synthesis of zeolite X at different temperatures (Hums et al. [31]).

## Experimental

Class F coal fly ash was supplied by ESKOM from a power plant located in the Mpumalanga province of South Africa. The fly ash was stored in sealed containers to preserve its compositional integrity. The mineralogical composition of fly ash, the fused fly ash and the crystallized products were determined by X-ray powder diffraction (XRD) using a Philips X-ray diffractometer with Cu-K $\alpha$  radiation and graphite monochromator. ICP-OES was used for the chemical characterization after digestion of 0.1 g sample in a solution of 8 ml HF, 2 ml HNO $_3$ , and 2 ml HCl. The morphology of the solid samples was studied using a scanning electron microscope with ultra-high resolution (FESEM, ULTRA 55 Carl Zeiss MST AG). The zeolites were synthesized from clear solution extracted from fused coal fly ash. This was achieved by initially grinding the fly ash with sodium hydroxide in a weight ratio of 1/2 using a ball mill for 20 min to obtain a fine homogeneously ground material. The resulting mixture was then fused at 550°C for 2 hours in a muffle furnace to convert insoluble fly ash mineral phases into soluble sodium silicate and sodium aluminate. The solid material was cooled down, crushed, dispersed in demineralized water in a weight ratio of 1/2.5 and stirred for 2 hours. The clear green solution extract obtained was separated from the insoluble material by filtration and subsequent centrifugation and then crystallized without stirring in polypropylene flasks at 70, 80 and 90°C for different times. The resulting zeolitic material was isolated by centrifugation, thoroughly washed with demineralized water until the pH of the washing water was below 9. The synthesis products were tried at 75°C overnight before characterization.

## Results and Discussion

The composition of raw fly ash was found to be mainly amorphous (62%) with the remaining crystalline phase consisting of quartz (13.5%), mullite (22.3%), hematite (1.6), and lime (0.5%) with a particle size <90 nm. After thermal fusion with sodium hydroxide the main mineral phases were sodium aluminate and sodium silicate; no evidence of quartz and mullite could be found as shown in [32]. Exemplarily for raw fly ash and fused fly ash SEM images are presented in [28]. The majority of the particles of the raw fly ash were observed to be spherical in shape related to the cooling effect of flue gas under power plant conditions. The predominantly spherical particles are transformed into an agglomerated porous mass after fusion. The fly ash used for this study showed insignificantly higher amounts of SiO $_2$  and Al $_2$ O $_3$  in comparison with the fly ash used in our previous study [28]. The XRD patterns of the samples obtained after crystallization and the corresponding reference diffractograms for zeolites A (LTA; pdf 00-038-0241), X (FAU; pdf 00-038-0237), P (GIS; pdf 00-040-1464), cancrinite (CAN; pdf 00-046-1332) and sodalite (SOD; pdf 00-037-0476) are shown in Figure 2. It can be seen that only reflections of zeolites A, X and SOD occur in the XRD patterns of samples a-d. Cancrinite, which is frequently reported to crystallize as an accompanying or consecutive phase of SOD [29,33] is not detected. According to the XRD results, hydrothermal treatment at 80°C for 25 hours (sample a) resulted in a mixture of zeolites A, X, and SOD. This is also stated by the corresponding SEM images in Figure 3a which show a mixture of particles with three different morphologies. The octahedral particles represent the typical morphology of zeolite X, zeolite A exhibits the typical cubic morphology and accordingly the thread-ball to armadillo-like clusters can be assigned to sodalite and not to a new morphology of hierarchical zeolite X as published in this context by Musyoka et al. [34-36]. When the crystallization at 80°C was extended from 25 hours (sample a) to 48 hours (sample b) the diffraction peaks of sodalite increased whereas the diffraction peaks of

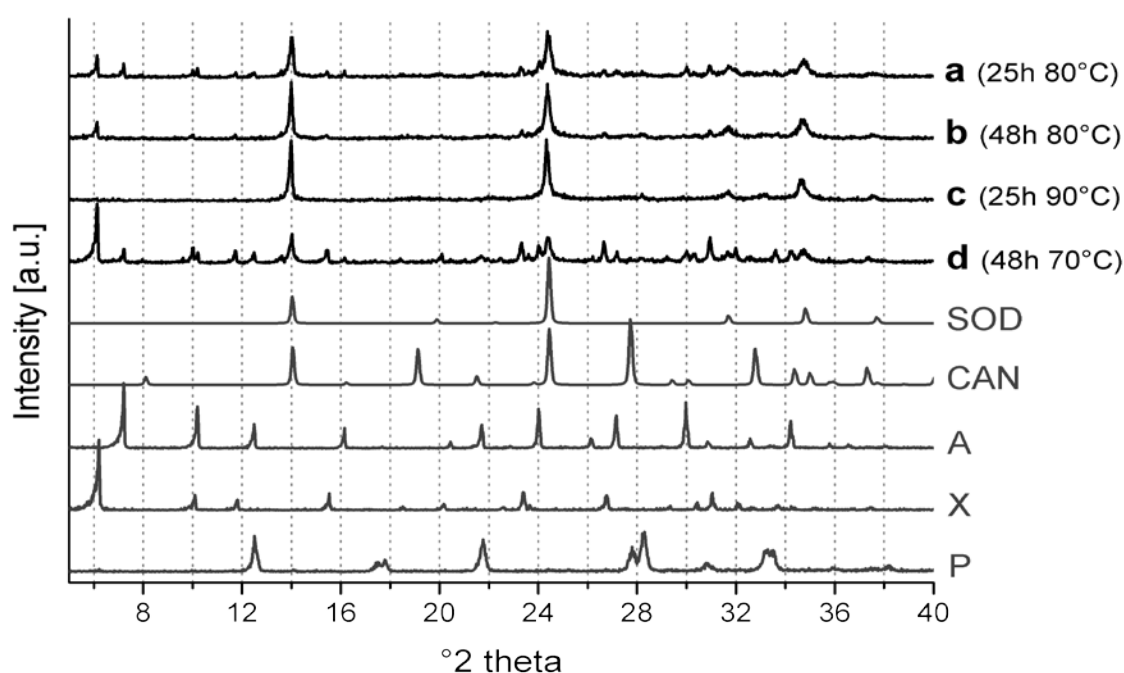


**Figure 2:** XRD patterns of the synthesis products from clear solution extract after crystallization at different reaction temperature and reaction time: at 80°C after 25 (sample a) and 48 hours (sample b); at 90°C after 25 hours (sample c), at 70°C after 48 hours (sample d) including the references for zeolites A, X, P, CAN, and SOD.

zeolite A disappeared, which is in agreement with the literature [32] and states that a phase transformation from zeolite A to sodalite took place. Also a decrease of the reflections of zeolite X can be observed, which correlates with the SEM images (Figure 3b), where a lower amount of octahedral zeolite X particles can be observed, whereas the amount of thread-ball-like and armadillo-like particles (SOD) increased. Also traces of zeolite A are still visible in the SEM images, but they start to be overgrown with SOD phase, which suggests that the transformation of LTA into SOD structure proceeds from the surface of the particles to the interior. The same mechanism seems to work for the transformation of zeolite X (FAU), because also zeolite X particles are overgrown with SOD phase (Figures 3a and 3b). The increase of the crystallization temperature from 80 to 90°C (sample c) accelerates the crystallization (and transformation) process and the XRD pattern (Figure 2) shows phase-pure SOD already after 25 h, whereas the reflections of zeolites X and A completely disappeared. Accordingly, the SEM images in Figure 3c show solely particles with armadillo-like morphology. However, two different sizes of SOD particles could be found during the SEM analyses of sample c (Figure 4). The large SOD particles seem to stem from the transformation of LTA or FAU zeolite particles, which is also evident from one SEM image where the armadillo-like phase seems to overgrow remaining particles of zeolite A or X (Figure 5c). In contrast, the smaller SOD particles might originate from SOD seeds which started to form and to grow later in the crystallization process. It is noticeable that two different types of SOD morphologies, namely thread-ball like and armadillo-like morphology, were observed depending on the crystallization conditions. The thread-ball-like SOD morphology accompanied the transformed particles of zeolites A and X and thus seemed to grow preferably on the surface of preformed zeolites (which also contain sodalite cages as the secondary building unit). This was also the case for the SOD impurities in zeolite X samples previously reported [30]. In contrast, the SOD particles growing from

SOD seeds had armadillo-like morphology. For the phase-pure SOD sample (sample c) it was observed that even the large SOD particles had the coarser armadillo-like morphology, suggesting that the thread-ball like morphology transformed into a more stable (less external surface) armadillo-like morphology. Different types of SOD morphologies were also found in the literature [28] where the morphology was influenced by several factors like NaOH concentration, type of anion, Si/Al ratio, salinity. Finally, a mix of cancrinite and sodalite was obtained by transformation of zeolite A [29,33]. Gualtieri et al. [37] also recognized that zeolite A is replaced by hydroxy-sodalite at higher crystallization temperatures and/or after longer heating periods. They suggested a nucleation of sodalite, because direct solid-state transformation of zeolite A to sodalite seemed impossible due to the large energy required to reform the double-four membered ring units. According to Subotic et al. [29] the transformation should be controlled by a solution-mediated process starting with the dissolution of zeolite A, followed by supersaturation of the synthesis solution and then heterogeneous nucleation as reason for the proposed phase transformation process. In the present study sodalite seems to nucleate close to the phase boundary of zeolite X via Ostwald ripening, proceeding from the surface to the inside of the particles as shown in the SEM images in Figure 5. Results of the elemental composition of the fly ash and the resulting phase-pure sodalite analysed by ICP are summarized in Table 1. It is important to be mentioned that the amount of foreign elements such as Ca, Fe, Ti and Ba in the final zeolite product is significantly reduced compared to the initial fly ash material.

## Conclusions

The present study showed that the clear solution extracted from South African type F fly ash exhibited a proper  $H_2O/SiO_2/Al_2O_3/NaOH$  ratio for the synthesis of zeolite sodalite without the need to

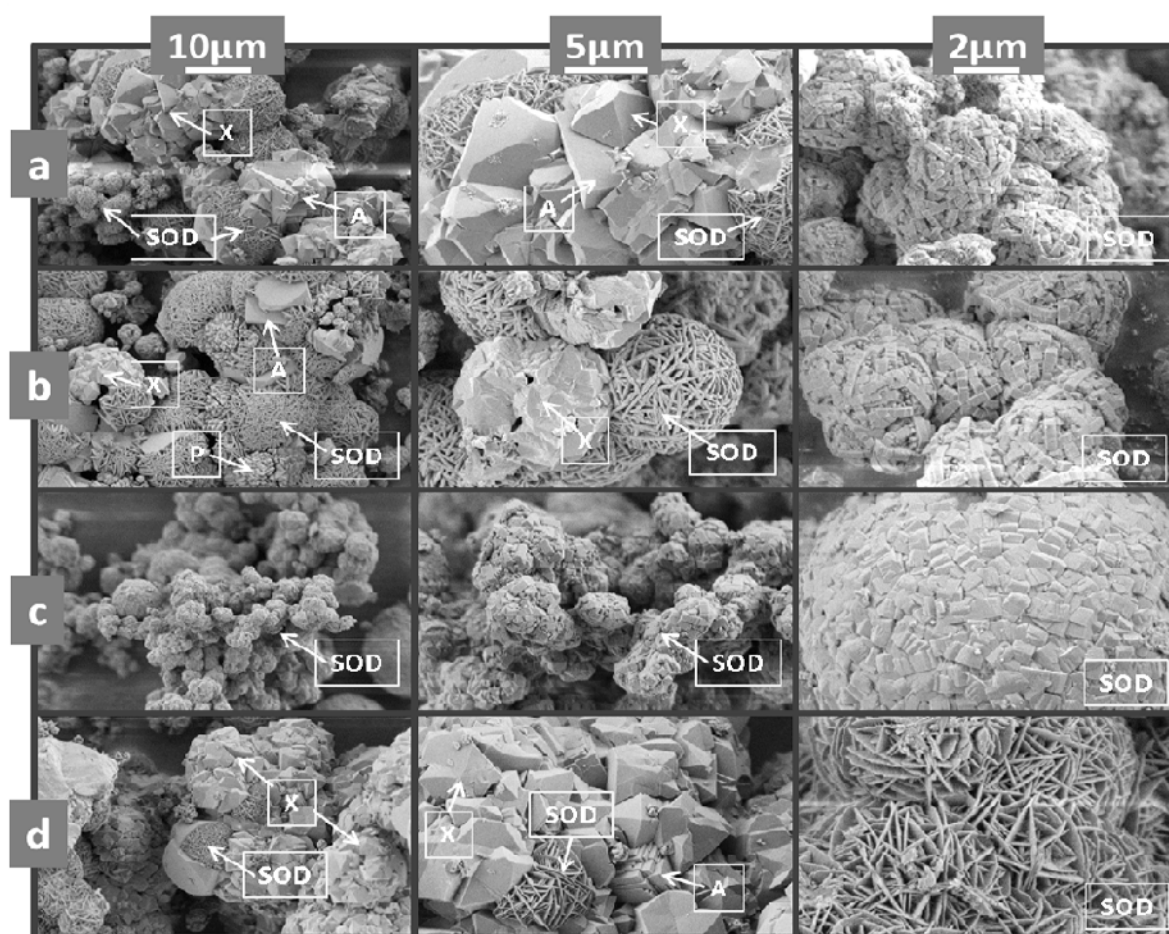


**Figure 3:** Selected SEM images corresponding to XRD patterns of the products synthesized at 80°C after 25 (sample a) and 48 hours (sample b), at 90°C after 25 hours (sample c) at 70°C after 48 hours (sample d).

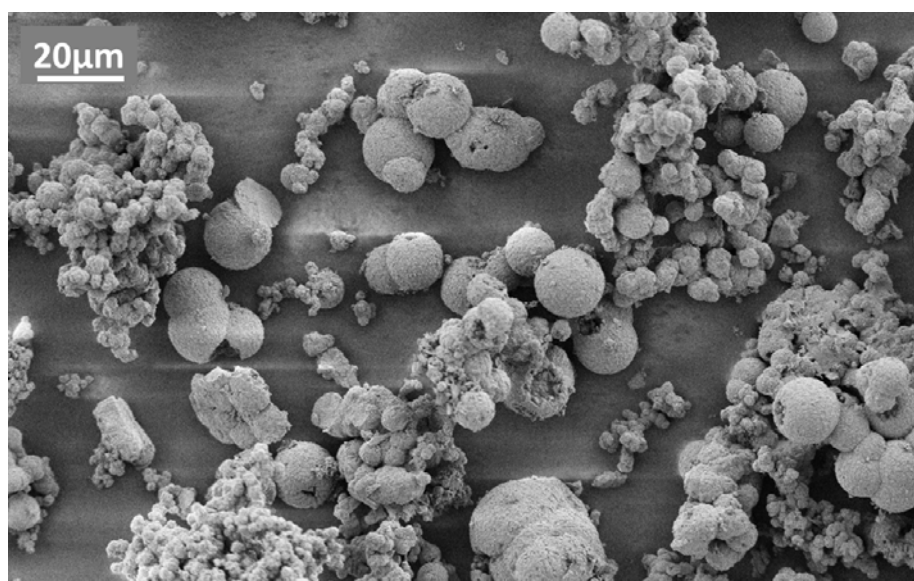


**Figure 4:** Overview: SEM image of different sizes of SOD.

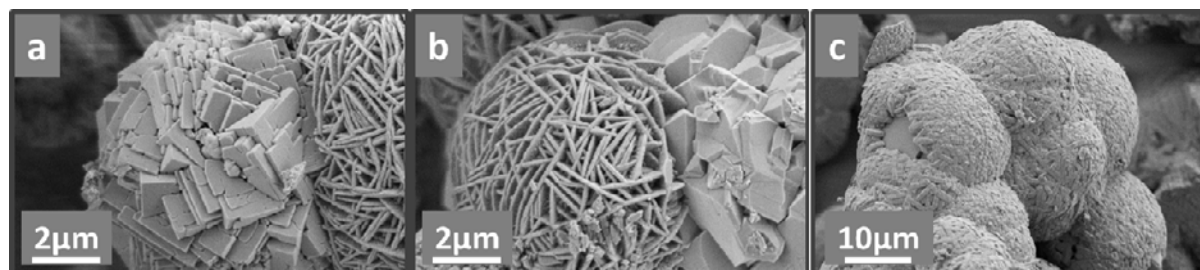


Figure 5: SEM images of armadillo-like phase overgrowing remaining particles of zeolite A and X showed by SEM images.

Element	Fly ash [wt-%] ICP	After crystallization [wt-%] ICP
Si	26.52	16.20
Al	14.53	11.00
Fe	3.46	0.38
Mn	0.01	0.01
Mg	0.62	0.01
Ca	1.47	0.04
Na	0.03	10.15
K	0.37	<0.22
Ti	0.93	<0.08
P	n.a.	0.09
S	n.a.	n.a.
Ba	0.00	0.00
Ce	n.a.	n.a.
Co	0.01	0.00
Cr	0.02	0.01
Cu	0.00	0.01
Li	0.01	n.a.
Mo	n.a.	<0.14
Nb	n.a.	n.a.
Ni	n.a.	0.01
Pb	n.a.	n.a.
Rb	n.a.	n.a.
Sr	n.a.	n.a.
Th	n.a.	n.a.
U	n.a.	n.a.
V	n.a.	0.00
Y	n.a.	n.a.
Zn	0.01	0.01
Zr	n.a.	n.a.

n.a.=not assigned

Table 1: ICP-OES results of elements of fly ash and synthesized sodalite from clear solution extracted from fused coal fly ash.

add any additional reactants. From XRD and SEM analyses it could be seen that (for the synthesis composition used) the crystallization of SOD, X and A is significantly affected by thermodynamic and kinetic parameters, from which finally zeolite SOD results. On this basis it was possible to suppress the formation of zeolites X and A by raising the crystallization temperature to 90°C. Furthermore, the morphology of the obtained SOD particles was found to vary with the crystallization conditions between thread-ball-like and armadillo-like. Since the zeolites were crystallized from the clear solution extracted from fused fly ash, there was no other solid material after crystallization except zeolite crystals. Also, the content of heavy metals in the product could be clearly reduced due to the lower content of heavy metals in the clear solution extract compared to the content of heavy metals in zeolites which were crystallized directly from fly ash [28]. However, it should be noted that with the procedure applied here, the yield of zeolite in respect to the amount of fly ash used is far away from an economically desirable quantity for the use of fused coal fly ash as industrial feedstock for zeolite syntheses. Nevertheless, in order to increase the yield of zeolite it seems promising to optimize the extraction step of the fused fly ash. Economically promising for a feasible scale-up option to synthesize zeolites is an approach to replace high temperature fusion by a short sonochemical treatment step in order to enrich aluminate and silicate in the clear solution extracted from fly ash. This technique is also profitable to reduce the ageing period and to increase the rate of crystallization [38,39].

#### Acknowledgements

The author would like to thank A. Inayat from the *University of Erlangen - Nürnberg, Germany* for performing experiments, A. Postatny to assist with ICP analyses and the German Research Foundation (DFG) and Prof. W. Schwieger for funding this study. Thanks, are also addressed to L. Petrik from the University of the Western Cape, South Africa for providing the fly ash from ESKOM for this project.

#### References

- Hums E, Baser H, Schwieger W (2016) In situ ultrasonic measurements: a powerful tool to control the synthesis of zeolites from coal fly ash. *Research on Chemical Intermediates* 42: 7513-7532.
- Hayashi S, Suzuki K, Shin S, Hayamizu K, Yamamoto O (1984) High-resolution solid-state NMR study of the crystallization of hydroxysodalite. *Chemical Physics Letters* 110: 54-57.
- Denk G, Menzel W (1971) Über die Reaktion von Kaolin mit Alkalilaugen. *Zeitschrift für anorganische und allgemeine Chemie* 382: 209-216.
- Subotić B, Škrtić D, Šmit I, Sekovanić L (1980) Transformation of zeolite A into hydroxysodalite: I. An approach to the mechanism of transformation and its experimental evaluation. *Journal of Crystal Growth*. 50: 498-508.
- Radhi AA. The Effects of Different Synthesis Conditions on Sodalite Crystal Morphology (Doctoral dissertation, Ohio University). Thesis 2001 Ohio University, USA.
- Huang Y, Yao J, Zhang X, Kong CC, Chen H, et al. (2011) Role of ethanol in

- sodalite crystallization in an ethanol–Na<sub>2</sub>O–Al<sub>2</sub>O<sub>3</sub>–SiO<sub>2</sub>–H<sub>2</sub>O system. *Cryst Eng Comm* 13: 4714-4722.
7. Borchert W, Keidel J (1947) Beiträge zur Reaktionsfähigkeit der Silikate bei niedrigen Temperaturen. *Heidelberger Beiträge zur Mineralogie und Petrographie* 1: 2-16.
  8. Barrer RM, White EA (1952) 286. The hydrothermal chemistry of silicates. Part II. Synthetic crystalline sodium aluminosilicates. *Journal of the Chemical Society (Resumed)* 1952: 1561-1571.
  9. Novembre D, Gimeno D, Pasculli A, Di Sabatino B (2010) Synthesis and characterization of sodalite using natural kaolinite: an analytical and mathematical approach to simulate the loss in weight of chlorine during the synthesis process. *Fresenius Environmental Bulletin* 19: 1109-1117.
  10. Ahmaruzzaman M (2010) A review on the utilization of fly ash. *Progress in energy and combustion science* 36: 327-363.
  11. Hums E (2008) Feasibility Study: Synthesis of zeolite from coal fly ash at a commercial scale in the context of fly ash leaching tests (2008 part of ESKOM project: Feasibility of Application of Zeolites made from Fly Ash).
  12. Singer A, Berggaut V (1995) Cation exchange properties of hydrothermally treated coal fly ash. *Environmental science & technology* 29: 1748-1753.
  13. Izidoro JD, Fungaro DA, dos Santos FS, Wang S (2012) Characteristics of Brazilian coal fly ashes and their synthesized zeolites. *Fuel Processing Technology* 97: 38-44.
  14. Musyoka NM, Petrik LF, Hums E, Baser H, Schwioger W (2012) In situ ultrasonic monitoring of zeolite A crystallization from coal fly ash. *Catalysis Today* 190: 38-46.
  15. Yao ZT, Li HY, Xia MS, Ye Y, Zhang L (2009) Hydrothermal synthesis of sodalite from coal fly ash and its property characterization [J]. *The Chinese Journal of Nonferrous Metals* 2: 030.
  16. Sodalit TB (2012) Characterization and Gravimetric Analysis of the Dissolved Quartz in the Conversion of Coal Fly Ash to Sodalite. *Malaysian Journal of Analytical Sciences* 16: 235-240.
  17. Maldonado M, Oleksiak MD, Chinta S, Rimer JD (2013) Controlling crystal polymorphism in organic-free synthesis of Na-zeolites. *Journal of the American Chemical Society* 135: 2641-2652.
  18. Molina A, Poole C (2004) A comparative study using two methods to produce zeolites from fly ash. *Minerals Engineering* 17: 167-73.
  19. Yaping Y, Xiaoqiang Z, Weilan Q, Mingwen W (2008) Synthesis of pure zeolites from supersaturated silicon and aluminum alkali extracts from fused coal fly ash *Fuel* 87: 1880-1886.
  20. Querol X, Moreno N, Umaña JT, Alastuey A, Hernández E, et al. (2002) Synthesis of zeolites from coal fly ash: an overview. *International Journal of coal geology* 50: 413-423.
  21. Querol X, Umama JC, Plana F, Alastuey A, Lopez-Soler A, et al. (2001) Synthesis of zeolites from fly ash at pilot plant scale. Examples of potential applications. *Fuel* 80: 857-865.
  22. Moriyama R, Takeda S, Onozaki M, Katayama Y, Shiota K, et al. (2005) Large-scale synthesis of artificial zeolite from coal fly ash with a small charge of alkaline solution. *Fuel* 84: 1455-1461.
  23. Moreno N, Querol X, Ayora C, Pereira CF, Janssen-Jurkovicová M (2001) Utilization of zeolites synthesized from coal fly ash for the purification of acid mine waters. *Environmental science & technology* 35: 3526-3534.
  24. Lee DB, Matsue N, Henmi T (2001) Influence of NaOH concentrations dissolved in seawater and hydrothermal temperatures on the synthesis of artificial zeolite from coal fly ash. *Clay science* 11: 451-463.
  25. Takashi H, Kazuharu Y (2008) Preparation of zeolitic adsorbents for environmental improvement from coal fly ash using alkali fusion. Downloaded by [217.229.39.141] at 10:18 21 May 2013 Waste brine used to synthesize hydroxy sodalite 1707 method. *Proceedings of the 3rd Japan - Taiwan Joint International Symposium on Environmental Science and Technology*. Kitakyushu, Japan.
  26. Belviso C, Cavalcante F, Lettino A, Fiore S (2009) Zeolite synthesised from fused coal fly ash at low temperature using seawater for crystallization. *Coal Combustion and Gasification Products* 1: 1-8.
  27. Musyoka NM, Petrik LF, Balfour G, Gitari WM, Hums E (2011) Synthesis of hydroxy sodalite from coal fly ash using waste industrial brine solution. *Journal of Environmental Science and Health, Part A* 46: 1699-1707.
  28. Musyoka NM, Petrik LF, Fatoba OO, Hums E (2013) Synthesis of zeolites from coal fly ash using mine waters. *Minerals Engineering* 53: 9-15.
  29. Deng Y, Harsh JB, Flury M, Young JS, Boyle JS (2016) Mineral formation during simulated leaks of Hanford waste tanks. *Applied Geochemistry* 21: 1392-1409.
  30. Subotić B, Škrtić D, Šmit I, Sekovanić L (1980) Transformation of zeolite A into hydroxysodalite: I. An approach to the mechanism of transformation and its experimental evaluation. *Journal of Crystal Growth* 50: 498-508.
  31. Subotić B, Sekovanić L (1986) Transformation of zeolite A into hydroxysodalite. II: Growth kinetics of hydroxysodalite microcrystals. *Journal of crystal growth* 75: 561-572.
  32. Hums E, Musyoka NM, Baser H, Inayat A, Schwioger W. In-situ ultrasound study of the kinetics of formation of zeolites Na–A and Na–X from coal fly ash. *Research on Chemical Intermediates* 41: 4311-4326.
  33. Hums E, Inayat A, Schwioger W (2016) Presentation, 18<sup>th</sup> International Zeolite Conference, Rio, Brazil.
  34. Reyes CA, Williams C, Alarcón OM (2013) Nucleation and growth process of sodalite and cancrinite from kaolinite-rich clay under low-temperature hydrothermal conditions. *Materials Research* 16: 424-438.
  35. Musyoka NM, Petrik LF, Hums E, Kuhnt A, Schwioger W (2015) Thermal stability studies of zeolites A and X synthesized from South African coal fly ash. *Research on Chemical Intermediates* 41: 575-582.
  36. Musyoka NM, Petrik LF, Hums E, Baser H, Schwioger W (2014) In situ ultrasonic diagnostic of zeolite X crystallization with novel (hierarchical) morphology from coal fly ash. *Ultrasonics* 54: 537-543.
  37. Musyoka NM, Petrik LF, Hums E (2016) Process for the Synthesis of Zeolites. PCT/IB2013/052438.
  38. Gualtieri A, Norby P, Artioli G, Hanson J (1997) Kinetics of formation of zeolite Na-A [LTA] from natural kaolinites. *Physics and Chemistry of Minerals* 24: 191-199.
  39. Musyoka NM, Petrik L, Hums E (2016) Inventors; Eskom Holdings Soc Limited, University of The Western Cape, Assignee. Ultrasonic synthesis of zeolites from fly ash. United States Patent US 9,522,828.